

See discussions, stats, and author profiles for this publication at: <https://www.researchgate.net/publication/223462144>

# Taking advantage of optical and electrical properties of organic molecules for gas sensing applications

ARTICLE *in* THIN SOLID FILMS · AUGUST 2001

Impact Factor: 1.76 · DOI: 10.1016/S0040-6090(01)01080-X

---

CITATIONS

24

---

READS

33

10 AUTHORS, INCLUDING:



[Kazunari Shinbo](#)

Niigata University

170 PUBLICATIONS 1,019 CITATIONS

SEE PROFILE



[Futao Kaneko](#)

Niigata University

220 PUBLICATIONS 1,521 CITATIONS

SEE PROFILE

## Taking advantage of optical and electrical properties of organic molecules for gas sensing applications

Tim H. Richardson<sup>a,\*</sup>, Colin M. Dooling<sup>a</sup>, Oliver Worsfold<sup>a</sup>, Liza T. Jones<sup>a</sup>,  
Keizo Kato<sup>b</sup>, Kazunari Shinbo<sup>c</sup>, Futao Kaneko<sup>c</sup>, Rose Treggoning<sup>d</sup>, M.O. Vysotsky<sup>d</sup>,  
Chris A. Hunter<sup>d</sup>

<sup>a</sup>*Applied Molecular Engineering Group, University of Sheffield, Hounsfield Road, Sheffield S3 7RH, UK*

<sup>b</sup>*Graduate School of Science and Technology, Niigata University, Niigata 950-2181, Japan*

<sup>c</sup>*Department of Electrical and Electronic Engineering, Niigata University, Niigata 950-2181, Japan*

<sup>d</sup>*Department of Chemistry, University of Sheffield, Brook Hill, Sheffield S3 7HF, UK*

### Abstract

The discipline of molecular electronics has grown rapidly over the last 10 years and is driven by the promise of the enhanced applied physical properties of functionalised organic materials compared to their inorganic partners. The subject can be divided generally into two broad themes, namely active molecular-scale electronics (or photonics), in which the control or generation of charge (or photons) at the nanoscale is attempted, and passive supra-molecular electronics (or photonics), in which the specific functionality of the molecules is modified by some interaction or process. In this paper, an example of the latter approach to molecular electronics will be given and this will describe the gas sensing properties of a tetra-substituted porphyrin molecule. The optical absorbance spectrum of LB film assemblies of 5,10,15,20-tetrakis(3,4-bis[2-ethylhexyloxy]phenyl)-21H,23H-porphine (EHO) is highly sensitive to low concentrations of NO<sub>2</sub>. LB films prepared at much faster than conventional deposition rates ( $\sim 1000$  mm min<sup>-1</sup>) yield  $t_{50}$  response and recovery times of 25 and 33 s, respectively, and show a sensitivity of 60% relative absorbance change (at 430 nm) for 4.4 ppm NO<sub>2</sub>. The morphology of these films is revealed using atomic force microscopy to contain isolated micron-size domains which are composed of grains of several nm in diameter. This unconventional structure leads to a useful sensing material as a result of the molecular functionality of the porphyrin coupled to the enhanced surface area of the porous film assembly. The EHO film shows a gradually diminishing optical response as its temperature is increased, resulting from the shift in the adsorption–desorption equilibrium towards desorption. The spectrum recovers fully after exposure to NO<sub>2</sub>. The rate of recovery is slow at room temperature but can be accelerated dramatically with gentle heating ( $\sim 350$  K) for a few seconds. The kinetics of the gas sensing process have been modelled and found to fit Elovichian surface adsorption for an initial fast surface adsorption process. This is followed by a much slower diffusive process in which the NO<sub>2</sub> molecules diffuse through the bulk of the assembly. The concentration dependence of the optical response over the range 0.8–4.4 ppm follows a Langmuir model. © 2001 Elsevier Science B.V. All rights reserved.

**Keywords:** Porphyrin; LB film; Langmuir–Blodgett; Gas sensor

\* Corresponding author. Tel.: +44-114-2824280; fax: +44-114-2728079.

E-mail address: t.richardson@sheffield.ac.uk (T.H. Richardson).

## 1. Introduction

The main disadvantages of the principal layer-by-layer deposition techniques, such as LB deposition [1] and poly-ion adsorption of polyelectrolytes [2], is the slow rate of substrate coverage that can be achieved. Traditionally, LB deposition involves linear deposition rates of typically  $1\text{--}50\text{ }\mu\text{m s}^{-1}$  per monolayer, and poly-ion adsorption rates correspond to complete monolayer formation in approximately 10–20 min per layer. Few attempts have ever been made to perform Langmuir film transfer at fast rates [3] and these have normally been limited to classical fatty acid materials. A recent development involved deposition at rates as high as  $1000\text{ }\mu\text{m s}^{-1}$  in order to produce ordered nano-channels in which novel chemistry can take place [4]. For at least one application — toxic gas sensing — highly homogeneous, ordered and dense molecular films are often actually detrimental in achieving good performance as a result of restricted access of the gas to the binding sites within the film. In this paper, ultra-fast deposition of a gas-sensitive porphyrin has been performed in order to produce semi-ordered aggregated assemblies that act as highly sensitive toxic gas sensors. The ability of monitoring toxic gases such as  $\text{NO}_2$ ,  $\text{Cl}_2$ ,  $\text{HCl}$ ,  $\text{SO}_2$ ,  $\text{H}_2\text{S}$ ,  $\text{CO}$  and  $\text{NH}_3$  in a wide range of environments has become very important over the last few years due to the increased toxic gas production in the chemical industry [5]. Ever more restrictive health, safety and environmental legislation has arisen that should ensure that human and environmental well-being are less effected by toxic substances [6]. This will only be confirmed if higher sensitivity gas sensors continue to be developed for monitoring at lower levels of concentration.

Most toxic gas sensors are based on semiconducting metal oxides [7] which function as a result of a gas-sensitive electrical conductivity and usually require relatively high operating temperatures ( $400\text{--}600^\circ\text{C}$ ). Other well-known sensor types include liquid electrolyte fuel cells and infra-red sensors [8]. Some attention has been guided towards organic materials as candidates for gas sensors. Certain conducting polymers [9] have achieved limited success in ‘electronic nose’ applications, and phthalocyanines have attracted interest as organic semi-conductometric sensors [10]. However, the majority of such organic sensors have exhibited relatively slow gas response time (typically in the range 5–10 min for  $t_{50}$ , the time taken for the measured sensor property to evolve to 50% of its final value) and incomplete recovery after gas exposure.

Porphyrins and their derivatives [11] have also been investigated although not as thoroughly as phthalocya-

nines. Recently a class of tetraphenyl porphyrins have shown promise as useful sensing materials [12]. Porphyrins are generally less conducting than most phthalocyanines but have the common property of possessing rich UV-visible absorption spectra owing to their highly conjugated  $\pi$ -electron systems [13]. The extended range of wavelengths now available as narrow-band light sources in the form of either light emitting diodes or laser diodes suggests that porphyrin assemblies deserve further study as potentially useful sensing materials.

## 2. Experimental

### 2.1. LB film preparation and AFM characterisation

The synthesis of EHO, whose chemical structure is shown in Fig. 1, has been reported elsewhere [14]. A Langmuir film of EHO was spread using chloroform ( $10^{-4}\text{ M}$ ) onto a clean water surface ( $\text{pH} \sim 6.2$ ,  $T = 296\text{ K}$ ). A silanising agent, 1,1,1-3,3,3 hexamethyldisilazane, was used to render pre-cleaned glass plates hydrophobic. Deposition was effected at an ultra-fast rate of  $1000\text{ mm min}^{-1}$ , using the maximum gain setting on a constant perimeter Langmuir trough, and a purpose built fast dipper mechanism (Nima Technology). Although not successful for all materials, such high transfer rates are compatible with EHO and certain other porphyrins and phthalocyanines [15,16]. Atomic force microscopy (AFM) was performed at room temperature in air using a Nanoscope IIIa (Digital Instruments) microscope in the tapping mode.

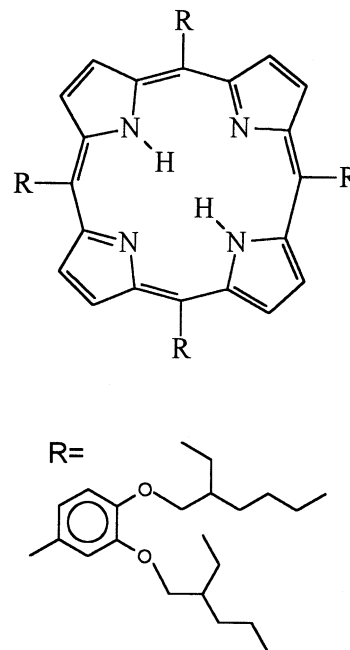


Fig. 1. Chemical structure of EHO.

## 2.2. Characterisation of optical gas response

A purpose built gas testing station depicted in Fig. 2 was used to assess the gas-sensitive optical properties of EHO films. This consisted of a gas delivery system incorporating two Tylan FC-260 mass flow controllers for determining the relative flows of toxic gas ( $\text{NO}_2$ ,  $\text{Cl}_2$ , or  $\text{HCl}$  as dilute mixtures in  $\text{N}_2$ ) and dry  $\text{N}_2$  (as a further diluent). The toxic gas cylinders (BOC UK) were obtained at nominally 5 ppm concentrations in dry  $\text{N}_2$ ; the delivery system facilitated the accurate production of diluted toxic gas in the concentration range 0.5–5.0 ppm (error estimated at 3%). This gas mixture was directed into a specially designed sealed gas testing chamber that held the EHO samples between two optical fibres originating and returning to the visible white light source and the multi-channel photodiode array detector, respectively. A World Precision Instruments Spectromate spectrophotometer was used to record visible absorption spectra over the wavelength range 350–850 nm at 3-s intervals throughout the gas exposure/recovery cycles. This instrument not only records entire spectra at each interval but displays absorbance data at preset wavelengths as a function of time, allowing convenient observation of the kinetics of the sensing process in real time. The temperature of the sample in the gas chamber could be altered over the range 285–363 K if required using a water-cooled

Peltier heating system. This was particularly useful during the recovery stage of each exposure/recovery cycle since elevated temperature was needed to obtain fast recovery as will be described later.

## 3. Results and discussion

### 3.1. Atomic force microscopy

Fig. 3 depicts an atomic force microscope image of a 10 excursion EHO assembly deposited at a rate of  $1000 \text{ mm min}^{-1}$  on to an optically flat hydrophobic glass substrate. One excursion represents a passage of the substrate downwards through the Langmuir film followed by its subsequent withdrawal out of the film. The image shows a morphology characterised by a disordered array of interconnecting porphyrin domains distributed over the surface. Typically each domain is of the order of  $1 \mu\text{m}$  in diameter. The underlying substrate can be seen between some of these domains and indeed the substrate has been imaged separately (not shown here) and has a surface roughness of  $\sim 0.3 \text{ nm}$ . From the height profile corresponding to this image, most importantly, the average height of the EHO domains is found to be  $\sim 55 \text{ nm}$ . This value is approximately twice as large as the expected value for the transfer of 20 monolayers (10 excursions) of the EHO Langmuir film; one might have expected a maxi-

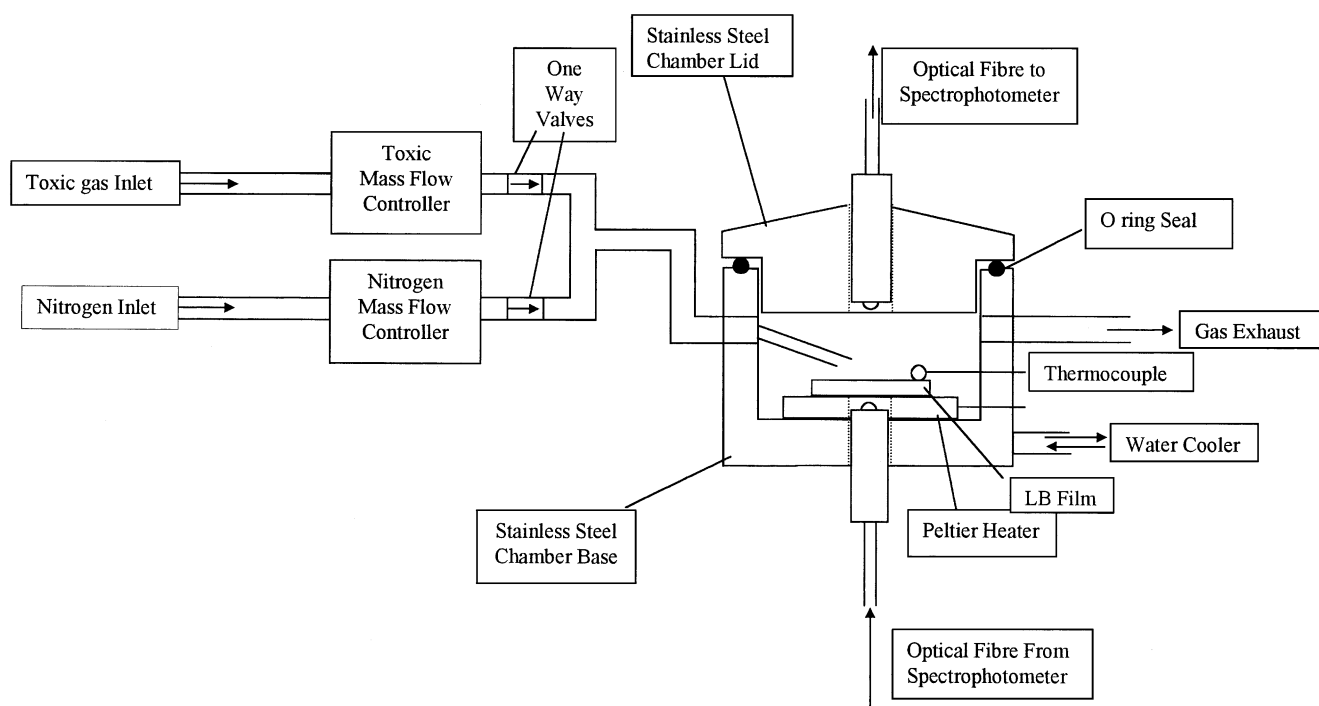


Fig. 2. Experimental arrangement for the gas testing station.

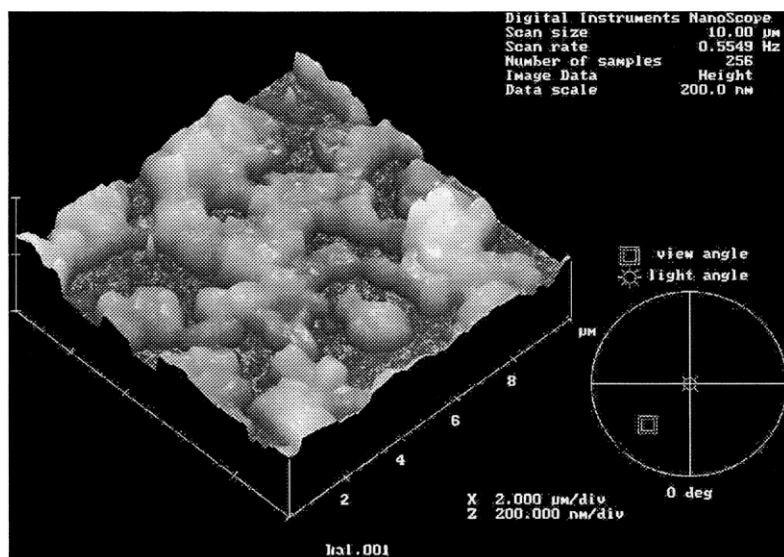


Fig. 3. Atomic force microscope image of an EHO LB film (10 excursions) deposited onto glass at a rate of  $1000 \text{ mm min}^{-1}$ .

imum value of  $\sim 26 \text{ nm}$  based on a thickness per monolayer of approximately  $1.3 \text{ nm}$  (corresponding approx. to the lateral dimension of the EHO porphyrin molecule). Although the morphology of the EHO assemblies shows that only approximately 40–50% of the substrate is coated, the transfer ratio measured by comparing the decrease in the floating film area with the area of the substrate passing through it was found to be 0.80. There are two possible interpretations of these data.

First, the partial substrate coverage may arise as a result of the co-transfer of a significant amount of water with (underneath) the porphyrin monolayer. This water layer may disassociate into many minute water droplets each covered by a section of the porphyrin monolayer. Evaporation of the water droplet would then allow the porphyrin layer to settle on the substrate. Subsequent depositions would involve porphyrin monolayer material preferentially settling on previously established porphyrin domains. This mechanism would provide one possible explanation for the island-type morphology and for the greater domain thicknesses measured by AFM. However, it should be noted that the only water seen to wet the substrate during deposition is a large droplet which adheres to the lowest part of the substrate — the majority of the coated substrates appear completely dry. The second interpretation relies on the island-type morphology existing within the floating film on the water surface itself. Thus, a perforated multilayer Langmuir film could be envisaged which is able to transfer onto a solid substrate at these ultra-fast deposition rates. Further work focused on establishing the deposition/growth mechanism will

involve Brewster angle microscopy to image the floating film morphology.

### 3.2. $\text{NO}_2$ sensitivity

The UV-visible absorbance spectrum of the EHO assembly changes during exposure to  $\text{NO}_2$  in a quite dramatic manner as indicated by Fig. 4. The characteristic absorbance spectrum of this porphyrin contains a sharp Soret band at  $434 \text{ nm}$  with satellite Q-bands at wavelengths in the range  $500\text{--}650 \text{ nm}$ . As a result of the exposure of this 3 excursion EHO assembly, the Soret band intensity decreases rapidly with a corresponding build up of optical density at  $475 \text{ nm}$  (strong) and  $700 \text{ nm}$  (weak). The mechanism for this  $\text{NO}_2$ –porphyrin reaction could be explained in terms of protonation of the central porphyrin core to form the porphyrin dication or oxidation to form a  $\pi$ -radical cation. Reports of the formation of both these species in metal-free and metalloporphyrins using acidic and electrophilic gases show that the resulting spectra are very similar [17–19]. In most cases, metalloporphyrins which are exposed to electrophilic gases such as  $\text{NO}_2$  and  $\text{Cl}_2$  yield a decreasing Soret band ( $\sim 430 \text{ nm}$ ) and increasing intensity at approximately  $700 \text{ nm}$ , but no absorbance band formation at  $460\text{--}480 \text{ nm}$ . It is thought that the metal atom effectively quenches protonation and that as a result only  $\pi$ -radical cation formation can occur through oxidation [19]. Furthermore, it is difficult to understand how the metalloporphyrin absorbance spectrum induced through gas exposure might reverse to its original pre-exposure form without further chemical reaction with a reducing species. As will be detailed shortly, in the case of EHO LB assemblies, full

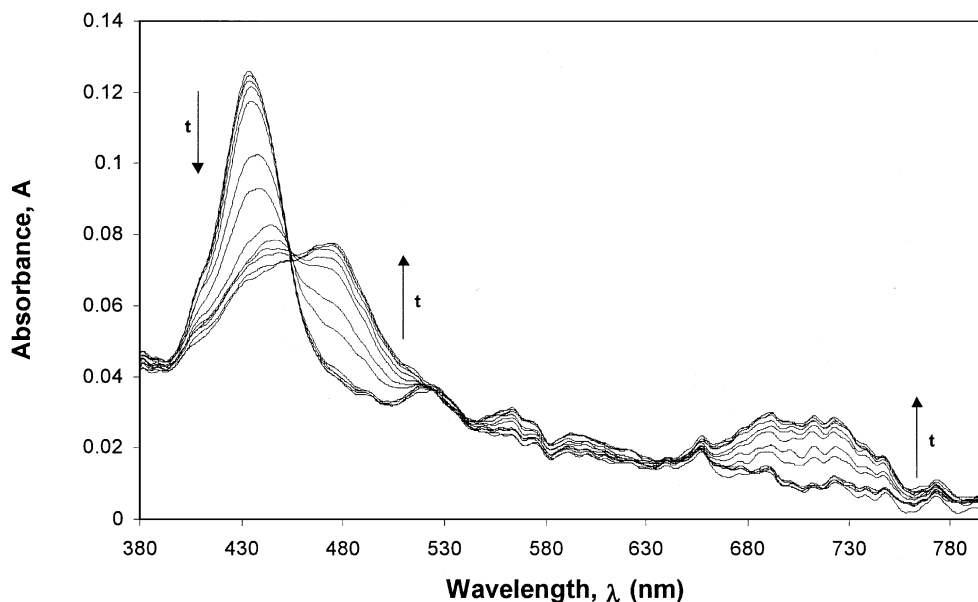


Fig. 4. Temporal development of the UV-visible spectrum of an EHO LB film (three excursions) during exposure to 4.4 ppm  $\text{NO}_2$  gas (time interval between spectra is 4 s).

recovery of the original spectrum is observed merely by flushing with dry nitrogen with moderate heating. In metal-free porphyrins, all three gases,  $\text{NO}_2$ ,  $\text{Cl}_2$  and  $\text{HCl}$  cause spectral changes similar to those observed in assemblies of EHO, namely a Soret band intensity reduction (434 nm), the appearance of a new strong band at 475 nm and a weak band at 720 nm [18]. These features, which are characteristic of protonation of the porphyrin core and the formation of a dication species, are expected when the porphyrin is exposed to  $\text{HCl}$ , but can only be readily explained in the cases of  $\text{NO}_2$  and  $\text{Cl}_2$  if adventitious water is also an active participant in the sensing mechanism. In the case of the EHO LB assemblies, dry gases are used at all times. Accordingly, the source of the water required to facilitate protonation may be the LB film itself. Future work will address this issue by studying the gas response of EHO assemblies stored at various relative humidity values.

The kinetics of the  $\text{NO}_2$  gas exposure (gas concentration = 4.4 ppm, sample temperature = 293 K) are shown in Fig. 5 in which the absorbance at the Soret wavelength (343 nm) is plotted as a function of time. This intensity falls rapidly immediately after the  $\text{NO}_2$  gas stream is switched on (occurring at 180 s), eventually saturating at an absorbance intensity 60% lower than the original level. At 1275 s, the  $\text{NO}_2$  gas stream is switched off and a dry nitrogen flush is activated whilst the sample is quickly heated to 353 K to initiate recovery. By 1433 s, the original Soret band intensity has been restored. Also shown in this figure are data corresponding to the gas response for a solution cast

film of EHO prepared from the spreading solution. It is notable that the observed response is initially much slower than the LB response, although the two rates do converge after a long time period. In the case of the solution, the crystallites formed (measured by optical microscopy) are approximately  $20 \times 20 \times 20 \mu\text{m}$  in dimension and are separated by enormous average distances of 40–80  $\mu\text{m}$ . The surface area to volume ratio therefore is very low compared to the case of EHO LB assemblies. It is expected therefore that the predominant process occurring in the solution cast film will be that of bulk diffusion into the large crystallites, whereas that in the LB film will be fast surface adsorption tempered by slow diffusion into EHO domains.

The decay of the Soret band absorbance has been found to fit Elovichian kinetics [10] readily. The Elovich model states that the rate of surface coverage ( $\Theta$ ) by the adsorbate gas is given by  $d\Theta/dt$  where

$$d\Theta/dt = A \exp\{-\beta\Theta\} \quad (1)$$

and  $A$ ,  $\beta$  are constants. This equation can be integrated to obtain an expression for the coverage itself in which

$$\Theta = (1/\beta) \ln(t) + K \quad (2)$$

in which  $K$  is also a constant. Therefore, the probability of adsorption of an  $\text{NO}_2$  gas molecule decreases exponentially as a function of the number  $\text{NO}_2$  molecules that have already adsorbed to the adsorbing surface. The plot of  $\Theta$  vs.  $\ln(t)$ , shown in Fig. 6, is

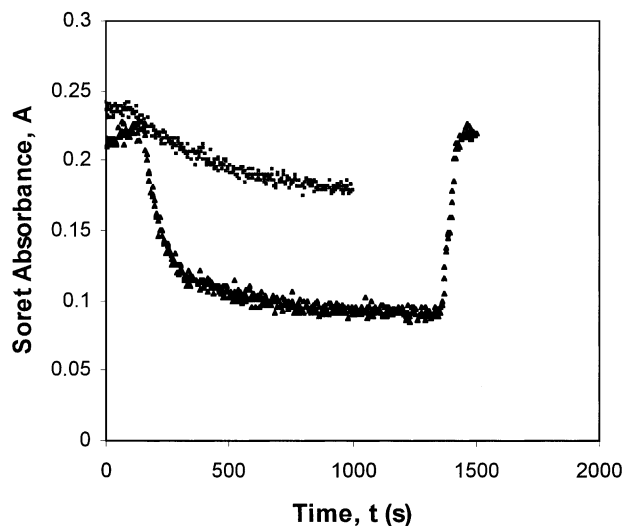


Fig. 5. Single exposure/recovery cycle for an EHO LB film assembly (lower plot) in comparison to the response of a solution cast film of EHO (upper plot) when exposed to 4.4 ppm  $\text{NO}_2$ . The solution curve has been normalised to the maximum absorbance of the LB film plot.

linear over the first 330 s of the exposure, deviating from linearity at higher time values. This behaviour is quite common in thin film organic sensing materials. The linear region represents surface adsorption in which  $\text{NO}_2$  molecules can adhere to the porphyrin binding sites at or very near the surface of the domains. However, diffusion into the ‘bulk’ of the domains is a much slower process due to steric hindrance and is represented by the slowly changing data on the right side of the Elovich plot which indicates that the surface adsorption is predominantly complete and that the diffusion process is still on-going.

The concentration dependence of the optical gas response for EHO assemblies is important to establish the sensitivity of the material for calibration purposes. Fig. 7 shows kinetics data for the concentration range 0.88–4.4 ppm  $\text{NO}_2$ . The response temperature was maintained at 293 K, but recovery was performed at 353 K. It is clear that the Soret band absorbance change converges as concentration increases even at these very low concentrations. Thus EHO assemblies are particularly useful in the very low concentration range up to 2000 ppb. Langmuir’s adsorption theory makes the assumptions that the activation energy for adsorption is the same for all binding sites in the thin film, that there is no adsorption of gas molecules striking sites on which an adsorbed  $\text{NO}_2$  molecule already resides (thus limiting adsorption at the surface to a single monolayer) and that there is no lateral motion of  $\text{NO}_2$  molecules over the surface. The theory indicates that a plot of  $\Delta\text{Abs}/c$  vs.  $c$  (where  $\Delta\text{Abs}$  is the change in the Soret band absorbance and  $c$  is the gas concentration) should be linear for Langmuir-type adsorption. Indeed, a highly linear relation is observed (Fig. 8) indicating that Langmuir adsorption, even with its limited assumptions, provides a basic understanding of the gas–porphyrin interaction during the sensing process. Further investigation into a wider range of adsorption/diffusion models will be made in the future.

#### 4. Summary

The principal conclusion is that, although the fast-dipping technique does not generate classical homogeneous, lamellar LB morphologies investigated for so

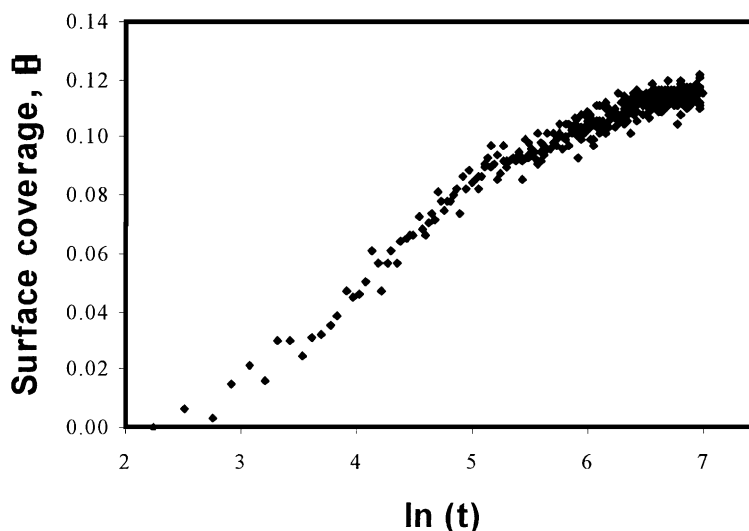


Fig. 6. Elovich response kinetics for a three-excursion EHO LB film (4.4 ppm).

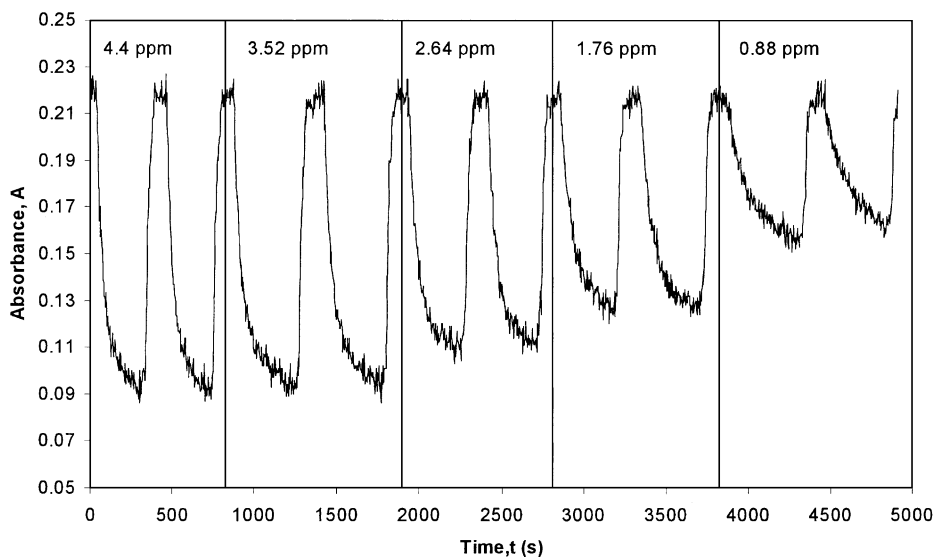


Fig. 7. Concentration dependence of an EHO LB film assembly over the range 0.8–4.4 ppm.

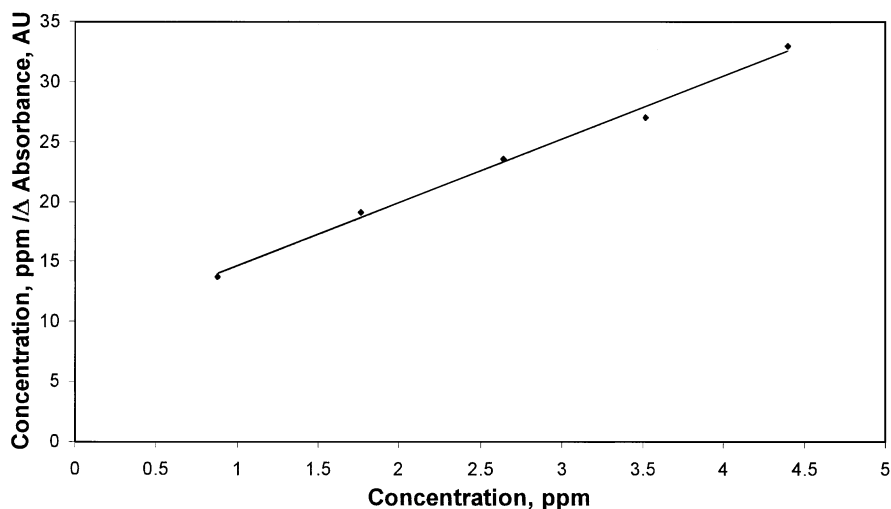


Fig. 8. Langmuir adsorption plot for an EHO LB film.

long by so many, nevertheless the disordered LB assemblies produced here have a very useful role to play in the development of new sensing materials.

## References

- [1] T.H. Richardson, *Functional Organic and Polymeric Materials*, Chichester, John Wiley & Sons, 2000.
- [2] G. Decher, Y. Lvov, J. Schmitt, *Thin Solid Films* 244 (1994) 772.
- [3] I.R. Peterson, G.J. Russell, G.G. Roberts, *Thin Solid Films* 109 (4) (1983) 371.
- [4] M. Gleiche, L.F. Chi, H. Fuchs, *Nature* 403 (6766) (2000) 173.
- [5] W. Gopel, J. Hesse, J.N. Zemel, *Sensors: A comprehensive survey, Chemical and Biochemical Sensors*, vol. 1 (2), VCH, 1991, p. 34.
- [6] R. Das, P.D. Blanc, *Toxicol. Ind. Health* 9 (1993) 439.
- [7] P.T. Moseley, J.O.W. Norris, D.E. Williams, *Techniques and Mechanisms in Gas Sensing*, Adam Hilger, Bristol, 1991.
- [8] W. Gopel, J. Hesse, J.N. Zemel, *Sensors: A comprehensive survey, Chemical and Biochemical Sensors*, vol. 1 (2), VCH, 1991, p. 313.
- [9] M.C. Lonergan, E.J. Severin, B.J. Doleman, S.A. Beaver, R.H. Grubb, N.S. Lewis, *Chem. Mater.* 8 (9) (1996) 2298.
- [10] S. Capone, S. Mongelli, R. Rella, P. Siciliano, L. Valli, *Langmuir* 15 (5) (1999) 1748.
- [11] T. Richardson, V.C. Smith, A. Topacli, J. Jiang, C.H. Huang, *Supramol. Sci.* 4 (3-4) (1997) 465.
- [12] T. Richardson, V.C. Smith, R.A.W. Johnstone, A.J.F.N. Sobral, A.M. d'A. Rocha Gonsalves, *Thin Solid Films* 327-329 (1998) 315.
- [13] L.R. Milgrom, *The Colours of Life*, Oxford University Press, Oxford, 1997.
- [14] O. Worsfold, L.T. Jones, C.M. Dooling, C.D. George, T.H. Richardson, M.O. Vysotsky, R. Tregonning, C.A. Hunter, C. Mailins, *J. Mater. Chem.* (submitted).



- [15] C.M. Dooling, T.H. Richardson, L. Valli, R. Rella, J. Jiang, *Colloid Surf. A: Physicochem. Eng. Aspects* (submitted).
- [16] M.B. Grieve, PhD Thesis, University of Sheffield, UK, August 1995.
- [17] J.P. Li, R.H. Tredgold, P. Hodge, *Thin Solid Films* 186 (1990) 167.
- [18] R. Bonnett, S. Ioannou, A.G. James, C.W. Pitt, M.M.Z. Soe, *J. Mater. Chem.* 2 (8) (1992) 823.
- [19] R. Bonnett, S. Ioannou, A.G. James, C.W. Pitt, M.M.Z. Soe, *J. Mater. Chem.* 3 (8) (1993) 793.